ARTICLE
Journal of Cellular Biochemistry 114:2039–2049 (2013)

Journal of Cellular Biochemistry

AKT Primes Snail-Induced EMT Concomitantly With the Collective Migration of Squamous Cell Carcinoma Cells

Gaku Okui, Kei Tobiume,* Andra Rizqiawan, Kazuhiro Yamamoto, Hideo Shigeishi, Shigehiro Ono, Koichiro Higashikawa, and Nobuyuki Kamata*

Department of Oral and Maxillofacial Surgery, Applied Life Sciences, Institute of Biomedical and Health Sciences, Hiroshima University, Hiroshima, Japan

ABSTRACT

In this study, we found that wounding of a confluent monolayer of squamous cell carcinoma (SCC) cells induced epithelial–mesenchymal transition (EMT) specifically at the edge of the wound. This process required the combined stimulation of TGFβ, TNFα, and PDGF-D. Such a combined cytokine treatment of confluent monolayers of the cells upregulated the expression levels of Snail and Slug via PI3K. The PI3K downstream effector, AKT, was dispensable for the upregulation of Snail and Slug, but essential for enabling EMT in response to upregulation of Snail and Slug. J. Cell. Biochem. 114: 2039–2049, 2013.

KEY WORDS: SQUAMOUS CELL CARCINOMA; EMT; SNAIL; AKT; PI3K

In a pool of freshly prepared cells expressing exogenous Snail via a retroviral vector to avoid clonal effects, only 20% of the growing cells displayed the epithelial–mesenchymal transition (EMT) phenotype. The population of cells undergoing EMT was diminished when the cells formed a confluent monolayer. However, upon wounding of the confluent monolayer, EMT was induced in the collectively migrating cells at the wound edge. Moreover, co-expression of a constitutively active AKT mutant with Snail increased the incidence of EMT concomitantly with the accelerated collective cell motility. Based on these findings, we conclude that the plasticity of Snail family-mediated EMT in squamous cell carcinoma (SCC) cells is regulated by the PI3K-AKT axis in response to the environmental condition.

Tumor cells within primary SCC exhibit various phenotypes even if the cell population shares the same oncogenic chromosomal alteration. When a cell undergoes the phenotypic change known as EMT in SCC, the cell loses its ability to bind to other cells via homophilic E-cadherin interactions, acquires a fibroblastic phenotype, and becomes invasive. Upon invasion of SCC cells into stromal tissue, it is assumed that the cells have undergone EMT.

EMT is typically characterized by spindle-shaped cells that cannot form homophilic cell–cell interactions because of the gain of a vimentin cytoskeleton and the loss of E-cadherin [Grünert et al., 2003; Kalluri and Weinberg, 2009]. Furthermore, EMT can be induced in several cancer cell types in vitro by exogenous expression of transcription factors (e.g., Snail, Slug, Zeb1, and Zeb2), and certain cytokines (e.g., TGFβ, TNFα, and PDGF-D) invoke a cell-type specific EMT program via the induction of these genes [Bakin et al., 2000; Cano et al., 2000; Comijn et al., 2001; Nieto, 2002; Zavadil et al., 2004; Barrallo-Gimeno and Nieto, 2005; Eger et al., 2005; Yang et al., 2006].

Snail is known to bind to and repress the promoter of the E-cadherin gene [Cano et al., 2000], and we previously found that the endogenous expression level of Snail correlates with the EMT phenotype of oral SCC cells [Yokoyama et al., 2001]. We were also able to induce EMT by exogenous expression of Snail in oral SCC cells [Yokoyama et al., 2003]. On the other hand, in SCC undergoing invasion, how Snail expression is regulated, and how EMT is differently regulated during the invasion and formation of a homophilic tumor cell nest are currently unknown.

The authors declare no conflict of interest.

Grant sponsor: Ministry of Education, Culture, Sports, Science and Technology, Japan; Grant numbers: 22249066, 21791823, 80363084.

*Correspondence to: Dr. Kei Tobiume and Nobuyuki Kamata, Department of Oral and Maxillofacial Surgery, Applied Life Sciences, Institute of Biomedical and Health Sciences, Hiroshima University, 1-2-3 Kasumi, Minami-ku, Hiroshima 734-8553, Japan. E-mail: tobi5651@hiroshima-u.ac.jp nokam@hiroshima-u.ac.jp

Manuscript Received: 12 February 2013; Manuscript Accepted: 13 March 2013

Accepted manuscript online in Wiley Online Library (wileyonlinelibrary.com): 29 March 2013

DOI 10.1002/jcb.24545 • © 2013 Wiley Periodicals, Inc.

Here, we report a novel mechanism that regulates EMT in oral SCC cells. Combined stimulation with TGFβ, TNFα, and PDGF-D upregulated the expression of Snail and Slug, whereas Snail/Slug-dependent EMT required PI3K-AKT-dependent polarized cell motility [Larue and Bellacosa, 2005] primed by wound formation in the confluent monolayer.

MATERIALS AND METHODS

CELLS AND REAGENTS

Human embryonic kidney cell lines HEK293gp (RCB, Tsukuba, Japan) and HEK293FT (Invitrogen, Carlsbad, CA, USA), and the human oral SCC cell line OM-1 [Taki et al., 2003] were cultured in Dulbecco's modified Eagle Medium (Sigma–Aldrich, St. Louis, MO, USA) supplemented with 10% fetal bovine serum (Biowest, Nuaillé, France). OM-1 cells expressing transgenes via retrovirus infection were maintained in medium containing 3 μg/ml puromycin (InvivoGen, San Diego, CA, USA) and 8 μg/ml blasticidin (InvivoGen). All cells were cultured in a humidified atmosphere with 5% CO_2 at 37°C.

Recombinant $TGF\beta_1$ and recombinant TNFα were obtained from PeproTech (Rocky Hill, NJ, USA). Recombinant PDGF-D was obtained from R&D Systems (Minneapolis, MN, USA). The MEK inhibitor PD98059 was purchased from Tocris Bioscience (Park Ellisville, MO, USA), and the NFκB inhibitor ammonium pyrrolidine dithiocarbamate (APDC) was purchased from Sigma–Aldrich. Rabbit monoclonal anti-Slug, anti-AKT, anti-phospho-AKT (Ser473), anti-p42/44 MAPK, anti-phospho-p42/44MAPK (Thr202/Tyr204), anti-IκBα, anti-phospho-IκBα (Ser32) and anti-E-cadherin antibodies, and the PI3K inhibitor LY294002 were purchased from Cell Signaling Technology (Boston, MA, USA). Other antibodies used in this study were mouse monoclonal anti-vimentin (Santa Cruz, Santa Cruz, CA, USA), anti-GAPDH (Millipore, Bedford, MA, USA) and anti-GFP (Nacalai Tesque, Kyoto, Japan).

RT-PCR

Total RNA was isolated using an RNeasy Mini Kit (Qiagen, Valencia, CA, USA) according to the manufacturer's protocol. cDNA was synthesized using ReverTra Ace (TOYOBO, Osaka, Japan). Semi-quantitative RT-PCR was performed with 30 cycles of denaturation at 95°C for 30 s, annealing for 30 s and extension at 72°C for 1 min. PCR primers were as follows:

. GAPDH-forward: 5′-ACCACAGTCCATGCCATCAC-3′
. GAPDH-reverse: 5′-TCC ACCACCCTGTTGCTGTA-3′
. Snail-forward: 5′-GCTGCAGGACTCTAATCCAGA-3′
. Snail-reverse: 5′-ATCTCCGGAGGTGGGATG-3′
. Slug-forward: 5′-GGGGAGAAGCCTTTTTCTTG-3′
. Slug-reverse: 5′-TCCTCATGTTTGTGCAGGAG-3′
. Zeb1-forward: 5′-GCTAGGCTGCTCAAGACTGAGT-3′
. Zeb1-reverse: 5′-GTGGCCCATTACAGGCAACCAGT-3′
. Zeb2-forward: 5′-CTCCAGGAGTAATACTCCTTCTCC-3′
. Zeb2-reverse: 5′-TAGGAAGCTCATCTGATCCAGTCC-3′
. Twist-forward: 5′-GTCCGCAGTCTTACGAGGAG-3′
. Twist-reverse: 5′-TGGAGGACCTGGTAGAGGAA-3′.

PCR products were separated by electrophoresis in 2% agarose gels and visualized by staining with ethidium bromide.

VIRAL VECTOR PLASMIDS

To construct pBabe-YFP/GW-puro, cDNA encoding YFP from pEYFP (Clontech, Mountain View, CA, USA) was cloned into pBabe-puro (Cosmo Bio, Tokyo, Japan) together with the gene fragment from a Gateway Vector Conversion Kit (Invitrogen) to create a new pBabe-based destination Gateway plasmid for C-terminal YFP tagging. Snail (GenBank accession number: AF155233) ORF cDNA was amplified from an OM-1 cDNA library using LA Taq with a GC Buffer kit (Takara Bio, Shiga, Japan), and then cloned into a pCR8 Gateway entry plasmid (Invitrogen) using a pCR8/GW/TOPO TA Cloning Kit (Invitrogen). Then, the entry vector was converted into pBabe-YFP/GW-puro and pLenti 6.2 DEST (Invitrogen). AKT1 (GenBank accession number EU332835) ORF cDNA was amplified from an OM-1 cDNA library using LA Taq with a GC Buffer kit, and then cloned into the *Bam*HI site of the pBabe-puro vector. Dominant negative AKT (AKT-K179R) in pBabe-puro was generated using a QuikChange Site-Directed Mutagenesis Kit (Stratagene, La Jolla, CA, USA). Constitutively active AKT (AKT-myr ΔPH) was prepared as described previously [Ramaswamy et al., 1999], and cloned into pBabe-puro.

RECOMBINANT VIRUS PRODUCTION AND INFECTION

The packaging plasmid pVSV-G and Virapower mix were purchased from Invitrogen. Virus host cells (HEK293gp or HEK293FT cells) were cotransfected with a viral vector plasmid (pBabe-puro or pLenti 6.2) and packaging plasmid (pVSV-G or Virapower mix) using a FuGENE6 (Roche, Basel, Switzerland). After 48 h, the viral supernatant containing 8 μg/ml polybrene (Sigma–Aldrich) was used to infect the target OM-1 cells by spinoculation.

WOUND HEALING ASSAY

Cells were seeded at a density of 1.5×10^5 cells/well in 24-well culture plates. A wound in the confluent monolayer was created by scraping with a 200 μl pipette tip. For immunoblotting and RT-PCR, multi-grid wounds were applied.

IMMUNOCYTOCHEMISTRY

Cells were seeded at a density of 1.5×10^5 cells/well (100% confluent) or 1×10^5 cells/well (70–80% confluent) in 24-well EZ View glass bottom LB culture plates (Iwaki, Tokyo, Japan). Wounding of confluent monolayers and stimulation with 5 ng/ml TGFβ [Medici et al., 2006], 10 ng/ml TNFα [Takahashi et al., 2010], and 20 ng/ml PDGF-D [LaRochelle et al., 2002] were performed at 24 h after plating. Cells were fixed in 4% paraformaldehyde in PBS for 15 min, followed by permeabilization with 0.2% Triton X-100 in PBS for 5 min and incubation with primary antibodies diluted in PBS containing 5% BSA for 8 h. Then, the cells were washed and incubated with diluted Alexa Fluor goat anti-mouse IgG (H + L) and Alexa Fluor goat anti-rabbit IgG (H + L) (Invitrogen) for 1 h. Vectashield anti-fade medium containing DAPI (Vector Laboratories, Burlingame, CA, USA) was used to mount the cells. Fluorescence and phase contrast images were acquired by a BZ-9000 microscope (KEYENCE, Osaka, Japan).

IMMUNOBLOTTING

Cells were harvested using a Mammalian Cell Lysis Kit (Sigma–Aldrich). Protein concentrations were determined using a protein assay kit (Bio-Rad Laboratories, Hercules, CA) and 25 μg of protein

from each sample was separated on 10% SDS-polyacrylamide gels. The separated proteins were transferred to Immobilon (Millipore) membranes that were blocked in 2% ECL Advance Blocking Reagent (GE Healthcare Bio-Sciences, Piscataway, NJ, USA) for 1 h at room temperature, and then incubated with a primary antibody diluted in TBS-T containing 5% BSA (Sigma–Aldrich) for 12 h at 4°C. After washing with TBS-T, the immunoblots were incubated with a HRP-conjugated secondary antibody (GE Healthcare Bio-Sciences) diluted in 2% ECL Advance Blocking Reagent. The immunoreactive bands were developed with an ECL Advance Western Blotting Detection Kit (GE Healthcare Bio-Sciences) and analyzed by a LAS 4000 mini imaging system (Fuji Film, Tokyo, Japan).

Densitometric analysis of immunoblots was performed using ImageJ software (National Institutes of Health, USA).

RNA INTERFERENCE

Transfection of short interfering RNAs (siRNAs) was performed in six-well culture plates according to the protocol recommended for Lipofectamine RNAiMAX (Invitrogen). The final concentration of siRNA used was 10 nM. The sequences of target-specific siRNA duplexes were as follows:

- si Snail sense: 5′-UGUAGCAGCCAGGGCCUAGAGAAGG-3′
- si Snail antisense: 5′-CCUUCUCUAGGCCCUGGCUGCUACA-3′
- si Slug sense: 5′-UGGAGUAACUCUCAUAGAGAUACGG-3′
- si Slug antisense: 5′-CCGUAUCUCUAUGAGAGUUACUCCA-3′.

STATISTICAL ANALYSIS

The Student′s *t*-test was used for comparison between two groups. Tukey′s test was used for multiple comparisons. Statistical differences were considered significant at $P < 0.01$. All statistical analyses were performed with Mathematica software (Wolfram Research, Champaign, IL, USA).

RESULTS

INDUCTION OF EMT VIA SNAIL IN OM-1 CELLS IS CONDITIONAL

Previously, we established homogenous cells with an EMT phenotype by transfecting a plasmid vector-carrying Snail into an oral SCC cell line with an epithelial phenotype [Yokoyama et al., 2003]. However, we noticed that not all single colonies harboring the Snail transgene contained homogenous cells that underwent EMT, suggesting that the response of OM-1 cells to Snail-dependent EMT is variable.

To further evaluate the consequences of exogenous Snail-mediated EMT induction, we freshly prepared a pool of OM-1 cells harboring the YFP-tagged Snail-transgene (OM-1 Snail pool) using a retrovirus vector, which prevented clonal effects because of its high gene transfer efficiency. When grown as single cell suspensions, the cells in the OM-1 Snail pool and control OM-1 cells expressing the YFP transgene formed colonies by homophilic cell–cell interactions (Fig. 1a), but spindle-shaped cells were observed specifically in the OM-1 Snail pool (Fig. 1a). The majority of cells in a given colony expressed exogenous Snail-YFP in their nuclei, but Snail-YFP was also localized in the cytoplasm of some cells (Fig. 1b).

Immunocytochemical analysis of growing cells in the OM-1 Snail pool with anti-E-cadherin and anti-vimentin antibodies demonstrated that 20% of the total cell population exhibited a typical EMT phenotype (i.e., negative for E-cadherin staining but positive for cytoskeletal vimentin staining). Some of the remaining cells were positive for both E-cadherin and cytoskeletal vimentin, while others expressed E-cadherin only (Fig. 1c). At confluency, almost all cells expressed E-cadherin at the plasma membrane, and we rarely observed spindle-shaped cells with cytoskeletal vimentin (Fig. 2a). These findings suggest that EMT in the individual cells of the Snail-OM-1 pool is variable and conditional, even when Snail is expressed constitutively in all cells. Furthermore, as shown by immunocytochemical staining (E-cadherin negative and vimentin positive), the population of cells that underwent EMT increased when proliferating cells in the OM-1 Snail pool were treated with TGFβ, TNFα, or PDGF-D (Fig. 2b,c). In particular, TNFα and PDGF-D obviously decreased the overall amount of E-cadherin in the total cell population (Fig. 2d), indicating that these cytokines enforce Snail-mediated suppression of the E-cadherin gene promoter.

COMBINED STIMULATION WITH TGFβ, TNFα AND PDGF-D FACILITATES EMT AT THE WOUND EDGE IN A CONFLUENT MONOLAYER OF OM-1 CELLS

Because TGFβ, TNFα, and PDGF-D possibly induced EMT independently of exogenous Snail expression in the OM-1 Snail pool, we examined whether proliferating wild-type OM-1 cells exhibited EMT following treatment with TGFβ, TNFα, and PDGF-D. Treatment with the individual cytokines or in combination failed to induce EMT in proliferating cells (data not shown). However, when a wound was made in a confluent monolayer, immunocytochemistry demonstrated that treatment with all three cytokines induced EMT at the edge of the wounded area (Fig. 3a). This effect was not apparent when the disappearance of E-cadherin was evaluated by immunoblotting because almost all cells except for those at the wound edge were quiescent rather than undergoing EMT (Fig. 3a,b). Although treatment with any two of the three cytokines did not induce the assembly of vimentin (as shown by immunocytochemistry), slight global upregulation of vimentin was detected by immunoblotting (Fig. 3b).

To determine which transcription factors induced EMT when a confluent monolayer of OM-1 cells was wounded, we examined mRNA expression profiles in response to the induction of EMT by TGFβ, TNFα, and PDGF-D. Snail mRNA expression was clearly induced during EMT in OM-1 cells (Fig. 3c). In accordance with the mRNA expression profiles, the expression of Snail protein was clearly increased from a low basal expression level by combined treatment with TGFβ, TNFα, and PDGF-D in confluent OM-1 cells (Fig. 3c). Slug protein expression was also upregulated slightly from the basal expression level (Fig. 3c). Combined treatment with all three cytokines activated AKT, NFκB, and ERK pathways, and wounding alone also enhanced AKT activity (Fig. 3c). To identify the signaling pathway essential for Snail and Slug upregulation, we used specific inhibitors for each pathway. As demonstrated in Figure 3c, specific suppression of PI3K, MEK, or NFκB by treatment with inhibitors was confirmed by the elimination of phospho-AKT and phospho-ERK, and attenuation of phospho-IκB degradation, respectively (Fig. 3c). Only the PI3K inhibitor suppressed the elevation of Snail and Slug levels (Fig. 3c), while ERK and NFκB pathways remained active. In contrast, the MEK inhibitor affected AKT and NFκB as well

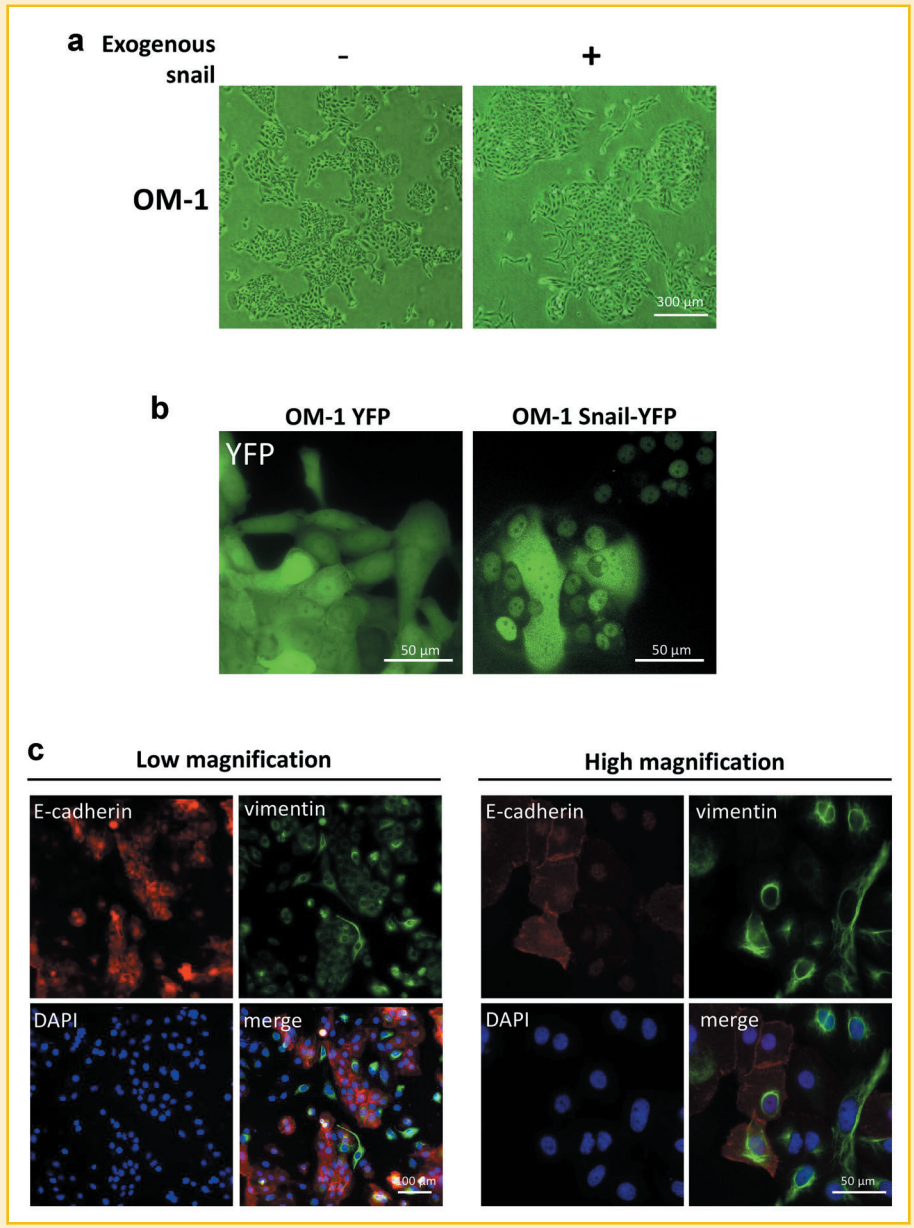

Figure 1. Heterogenous populations of growing cells from the freshly prepared OM-1 Snail pool. a: Morphology of growing cells in the OM-1 YFP pool (left) and OM-1 Snail-pool (right). b: Localization of transgenic Snail-YFP in cells of the OM-1 YFP pool (left) and OM-1 Snail pool (right). c: Immunocytochemical analysis of growing cells in the OM-1 Snail pool. Bound anti-E-cadherin antibody was visualized with Alexa Fluor 488-conjugated anti-rabbit IgG that was artificially colored as red in images using BZ-H2A imaging software. The Snail-YFP signal is also shown as red in the same view (top left), confirming that all cells in the view expressed Snail-YFP. The anti-vimentin antibody was visualized with Alexa Fluor 568-conjugated anti-mouse IgG that was artificially colored as green in images. Nuclei were visualized with DAPI and are displayed as blue.

as ERK, but Snail and Slug remained unaffected (Fig. 3c), indicating that PI3K regulates Snail and Slug expression independently of AKT status.

TNFα ENHANCES THE NUCLEAR LOCALIZATION OF SNAIL

We next examined the individual effects of TGFβ, TNFα, or PDGF-D on Snail/Slug induction and EMT in wounded confluent monolayers of OM-1 cells. As shown in Figure 4a, stimulation with the individual cytokines failed to induce EMT. However, accelerated cell migration in the absence of disturbed homophilic cell–cell interactions was observed in PDGF-D-treated cell cultures (right middle and bottom panels). Some cells displayed higher vimentin staining concomitant with E-cadherin staining, but the staining pattern was not indicative of a filamentous cytoskeleton. In particular, among TNFα-treated cells (right top panel and left middle panel), cells with a protruded cell body but without a vimentin cytoskeleton appeared at the wound edge. Treatment with TGFβ or TNFα alone clearly increased the expression levels of Snail and Slug (Fig. 4b). Treatment with TGFβ alone was particularly able to induce Snail at a level similar to that observed when the cells underwent EMT after wounding of the

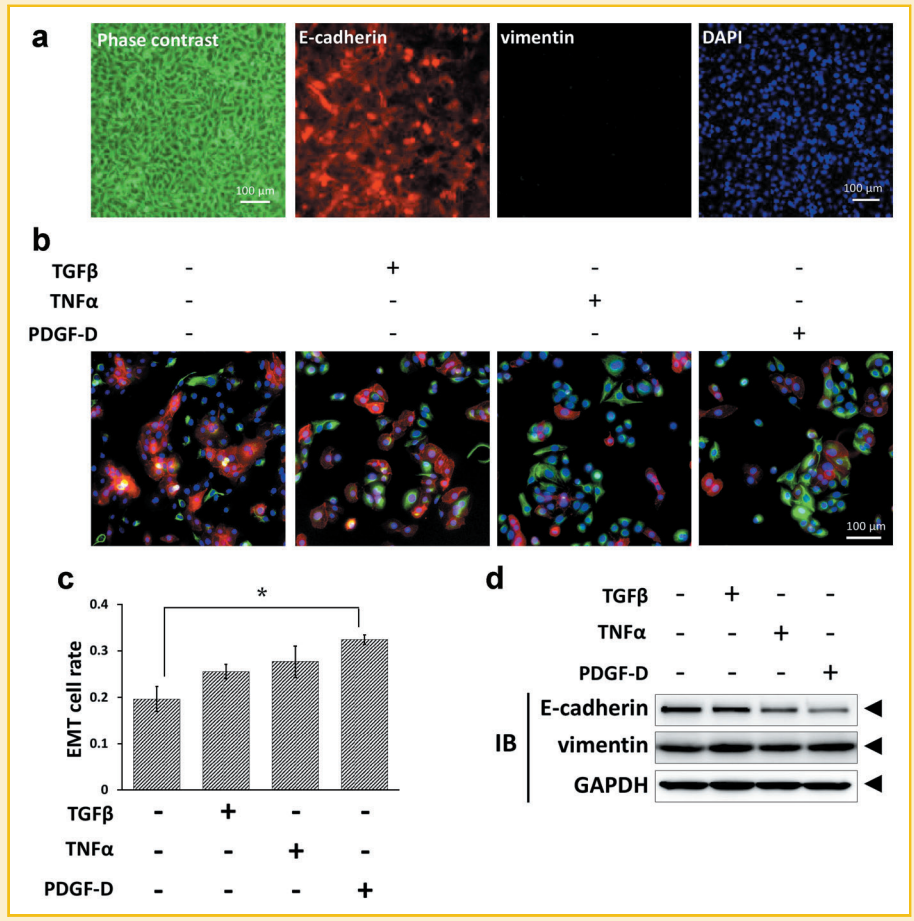

Figure 2. EMT in the OM-1 Snail pool is conditional. Immunocytochemical analysis of E-cadherin and YFP-snail (red), vimentin (green), and nuclei (blue) in the OM-1 Snail pool under various culture conditions. a: A confluent OM-1 Snail pool monolayer showing no vimentin-positive cells in a low power field. b: Growing OM-1 cells in the Snail pool cultured in the presence of TGFβ (5 ng/ml), TNFα (10 ng/ml), or PDGF-D (20 ng/ml) for 24 h. c: The rate of EMT in (b) was determined by counting the number of cells. The cells with a cytoskeletal pattern of vimentin staining were counted as vimentin positive. Cells negative for E-cadherin but positive for vimentin were defined as EMT. Each rate is represented as the mean of six independent fields. Error bars represent the SE. $^{*}P < 0.01$, Tukey's test. d: Immunoblot analysis of E-cadherin, vimentin and GAPDH in whole cell extracts from the cultured cells shown in (b). Densitometric analysis with statistical evaluation among three independent immunoblots is shown in Supplementary Figure 1a.

monolayer in the presence of TGFβ, TNFα, and PDGF-D (Fig. 4b). In contrast, AKT was activated by TGFβ and PDGF-D, but not TNFα (Fig. 4b). TGFβ-dependent Snail expression was also confirmed by immunocytochemical staining for endogenous Snail (Fig. 4c). Although TNFα-dependent upregulation of Snail was not apparent in immunocytochemistry (Fig. 4c), Snail clearly accumulated in the nuclei of TGFβ-treated cells after TNFα treatment (Fig. 4c).

These results suggest that TGFβ signaling is sufficient for induction of Snail/Slug expression, but insufficient to induce cells on the edges of the wound to undergo EMT, indicating augmented effects of the combined cytokines on Snail/Slug induction and promotion of cell migration in the monolayer upon EMT.

DOUBLE KNOCKDOWN OF SNAIL AND SLUG ATTENUATES CYTOKINE-DEPENDENT EMT AT THE WOUND EDGE IN A MONOLAYER OF OM-1 CELLS

To evaluate the functional contribution of cytokine-dependent induction of Snail and Slug expression to wound-induced EMT in the OM-1 cell monolayer, we next performed gene silencing of Snail and Slug expression. In cells transfected with siRNAs specific for Snail and Slug, the expression of both target genes was efficiently suppressed (Fig. 5a). When the cells were co-transfected with both siRNAs, cytokine-dependent EMT at the wound edges in the monolayer was completely suppressed (Fig. 5a,b), and the wound area remained the same width as that in a cell monolayer without cytokine treatment (Fig. 5d). In contrast, neither Snail- nor Slug-depleted OM-1 cells significantly underwent EMT, but exhibited EMT at the edges of the wounds in monolayer cultures where closure of the wound was slightly delayed (Fig. 5d). These results confirmed that upregulation of Snail and Slug expression is required for topical cytokine-dependent EMT at the wound edge in monolayer cultures of OM-1 cells.

PI3K SIGNALING INCREASES THE INCIDENCE OF EMT CONCOMITANTLY WITH COLLECTIVE CELL MIGRATION

Next, we determined which signaling pathways were associated with EMT induced by the three cytokines. As expected based on PI3K-dependent Snail induction in OM-1 cells treated with all three cytokines (Fig. 3c), PI3K inhibition completely suppressed EMT at the wound edge (Fig. 6a). While the suppression of Snail induction was

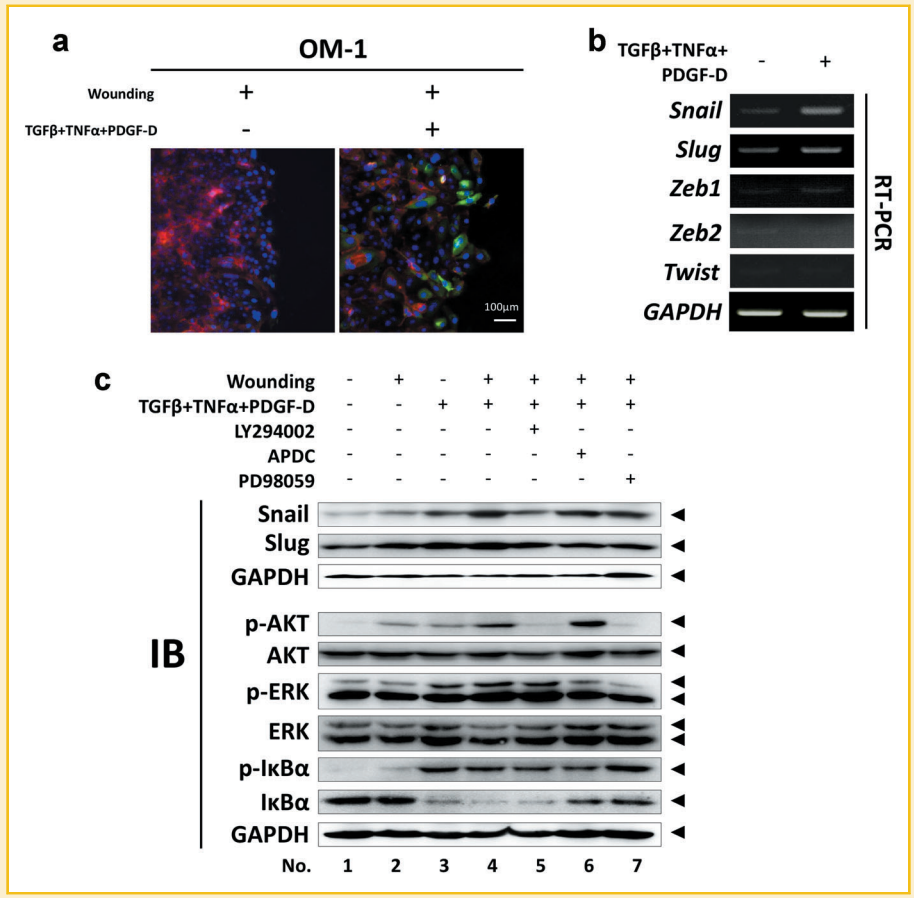

Figure 3. Wild-type OM-1 cells in confluent monolayers undergo wound-induced EMT in response to TGFβ, TNFα, and PDGF-D treatment. A confluent monolayer of OM-1 cells was cultured in the presence of TGFβ, TNFα, and PDGF-D for 24 h after wounding (see Materials and Methods Section). a: Immunocytochemical analysis of wound edges in a confluent monolayer of OM-1 cells (red: E-cadherin; green: vimentin; blue: nuclei) showing that wounding alone did not induce EMT (right). Wounded cells underwent EMT following simultaneous stimulation with TGFβ, TNFα, and PDGF-D (left). Anti-E-cadherin and anti-vimentin antibodies were visualized using Alexa Fluor 568-conjugated anti-rabbit IgG and Alexa Fluor 488-conjugated anti-mouse IgG, respectively. Nuclei were visualized with DAPI. b: mRNA expression profiles for the indicated genes in a wounded monolayer of OM-1 cells. The cells were harvested at 3 h after treatment with the indicated stimuli. c: Protein expression and signaling pathway profiles of OM-1 cells treated with the indicated stimuli. PI3K inhibitor LY294002 (50 μM), MEK inhibitor PD98059 (20 μM), and NF-kB inhibitor APDC (20 μM) were added to confluent OM-1 cell cultures at 1 h prior to application of stimuli and wounding. Snail and Slug expression was analyzed after incubating the cells for 3 h under the indicated conditions. To evaluate the phosphorylation status of signaling molecules, cells were harvested after 30 min of stimulation. Densitometric analysis with statistical evaluation among three independent immunoblots is shown in Supplementary Figure 1b and c.

incomplete (Fig. 3c), both NFκB and MEK inhibition significantly decreased the number of cells undergoing EMT at the wound edge (Fig. 6a,b), and wound closure was also delayed (Fig. 6c). In contrast, PI3K inhibition completely suppressed the collective migration of cells without cytokine treatment at 24 h (Fig. 6c), suggesting that PI3K signaling also plays a fundamental role in collective cell migration as well as inducing Snail family proteins. Therefore, we evaluated the specific role of PI3K in Snail-mediated EMT by adding a PI3K inhibitor to the OM-1 Snail pool. OM-1 Snail pool cells in a confluent monolayer displayed re-emergence of EMT at the edge of the wound in the absence of cytokine treatment, which was suppressed by the PI3K inhibitor (Fig. 6d,e). As demonstrated by diminished vimentin expression on immunoblots (Fig. 6f), the PI3K inhibitor also suppressed the incidence of EMT in the growing OM-1 Snail pool. These results indicate that EMT in Snail-expressing SCC cells coincides with collective cell mobility under PI3K signaling.

AKT-SIGNALING INCREASES THE INCIDENCE OF EMT IN SNAIL-ELEVATED CELLS

As demonstrated in Figure 3c (lanes 5 and 7), PI3K was essential for the induction of Snail and Slug in response to combined treatment with TGFβ, TNFα, and PDGF-D, but downstream AKT activation was dispensable for induction of these proteins. To better understand the correlation between AKT activation and the induction of Snail and Slug following combined treatment with TGFβ, TNFα, and PDGF-D, we tested the responses of confluent monolayers of OM-1 cells to the cytokines at various times after wounding. As shown in Figure 7a, delayed addition of the three cytokines after wounding induced Snail and Slug in the absence of AKT activation (lanes 5 and 6). In contrast, wounding and simultaneous cytokine stimulation enhanced the wound-induced activation of AKT (lanes 1 and 2). Moreover, depletion of the three cytokines by changing the culture medium clearly diminished the expression levels of Snail and Slug (lane 9),

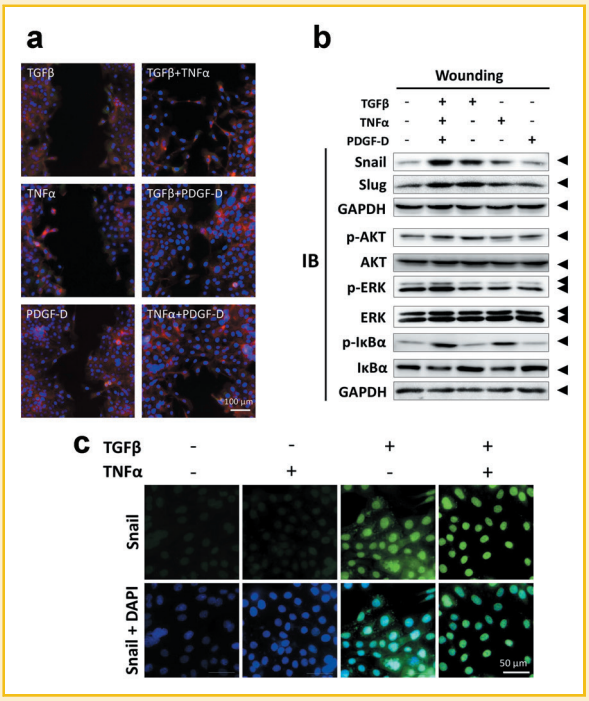

Figure 4. Treatment with TGFβ, TNFα, or PDGF-D alone is not sufficient for wound-induced EMT in confluent OM-1 cells. a: Confluent OM-1 cells were wounded and stimulated with the indicated cytokines. Immunocytochemistry was performed at 24 h after wounding (red: E-cadherin; green: vimentin; blue: nuclei). b: Immunoblotting of the differentially stimulated confluent OM-1 cells with the indicated antibodies. Densitometric analysis with statistical evaluation among three independent immunoblots is shown in Supplementary Figure 2a and c (c) Immunocytochemical analysis of endogenous Snail in OM-1 cells treated with the indicated stimuli for 3 h. The signal from the anti-Snail antibody was visualized using Alexa Fluor 488-conjugated anti-rabbit IgG. Nuclei were visualized with DAPI. All images were captured with the same exposure time (0.5 s).

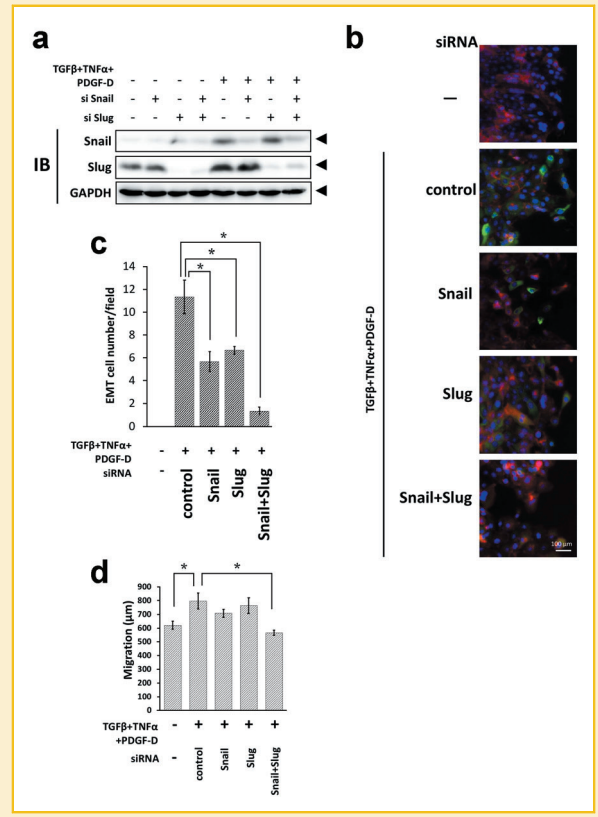

Figure 5. Snail and Slug are essential for wound-induced EMT in response to combined stimulation with TGFβ, TNFα, and PDGF-D. a: Immunoblot analysis of whole cell extracts from OM-1 cells treated with the indicated stimuli. At 24 h after transfection with the indicated siRNAs, confluent OM-1 cells were cultured in the presence or absence of combined stimulation with TGFβ, TNFα, and PDGF-D for 3 h. Densitometric analysis with statistical evaluation among three independent immunoblots is shown in Supplementary Figure 2c. b: Immunocytochemical analysis of a wounded confluent monolayer of OM1 cells. At 24 h after transfection with the indicated siRNAs, confluent OM-1 cells were wounded and cultured in the presence or absence of combined stimulation with TGFβ, TNFα, and PDGF-D for 24 h (red: E-cadherin; green: vimentin; blue: nuclei). c: The rate of EMT in (b) was determined as described in Figure 2c. Data are represented as the means of six independent fields with the SE. $^{*}P < 0.01$, Tukey's test. d: Statistical analysis of wound closure in (b). The distance migrated was measured in phase contrast microscopic views. Data are represented as the means of six independent fields. Error bars represent the SE. $^{*}P < 0.01$, Tukey's test.

indicating a reduced contribution of AKT to the cytokine-dependent upregulation of Snail and Slug.

To clarify the role of AKT for EMT in response to combined treatment with TGFβ, TNFα, and PDGF-D, we freshly generated OM-1 cells expressing either dominant negative AKT (AKT-DN) or constitutively active AKT (AKT-CA) [Ramaswamy et al., 1999]. Induction of Snail and Slug was not attenuated by AKT-DN in response to combined stimulation with TGFβ, TNFα, and PDGF-D (Fig. 7b), whereas vimentin induction concomitant with EMT was completely abolished (Fig. 7b,d). AKT-CA had no effect on Snail and Slug expression levels (Fig. 7b), confirming a negligible effect of AKT on Snail and Slug induction under PI3K signaling. However, co-expression of AKT-CA markedly increased the incidence of EMT in OM1 cells expressing exogenous Snail (Fig. 8a,b), which was insensitive to the PI3K inhibitor (Fig. 8a,b). AKT-CA also facilitated collective cell migration (Fig. 8c), whereas AKT-DN suppressed the collective migration of OM1 cells in a monolayer at 24 h after wounding (Fig. 7c). However, combined cytokine treatment with TGFβ, TNFα, and PDGF-D resulted in a greater incidence of EMT than that of AKT-CA-dependent EMT, indicating that these cytokines also promote EMT using pathways other than AKT signaling (Fig. 8a,b).

Taken together, we conclude that AKT activation primes EMT, which is in parallel with Snail/Slug induction in the downstream of the PI3K signaling (Fig. 8d).

DISCUSSION

Oral SCC cells with a constitutive EMT phenotype express EMT master transcription factors such as Snail at high levels [Yokoyama et al., 2001]. EMT promotes local invasion and metastasis, and is strongly associated with cancer prognosis [Thiery et al., 2009]. Upon local colonization following disruption of the basement membrane barrier or distant colonization following extravasation from the circulatory system during the cancer life cycle, cancer cells acquire

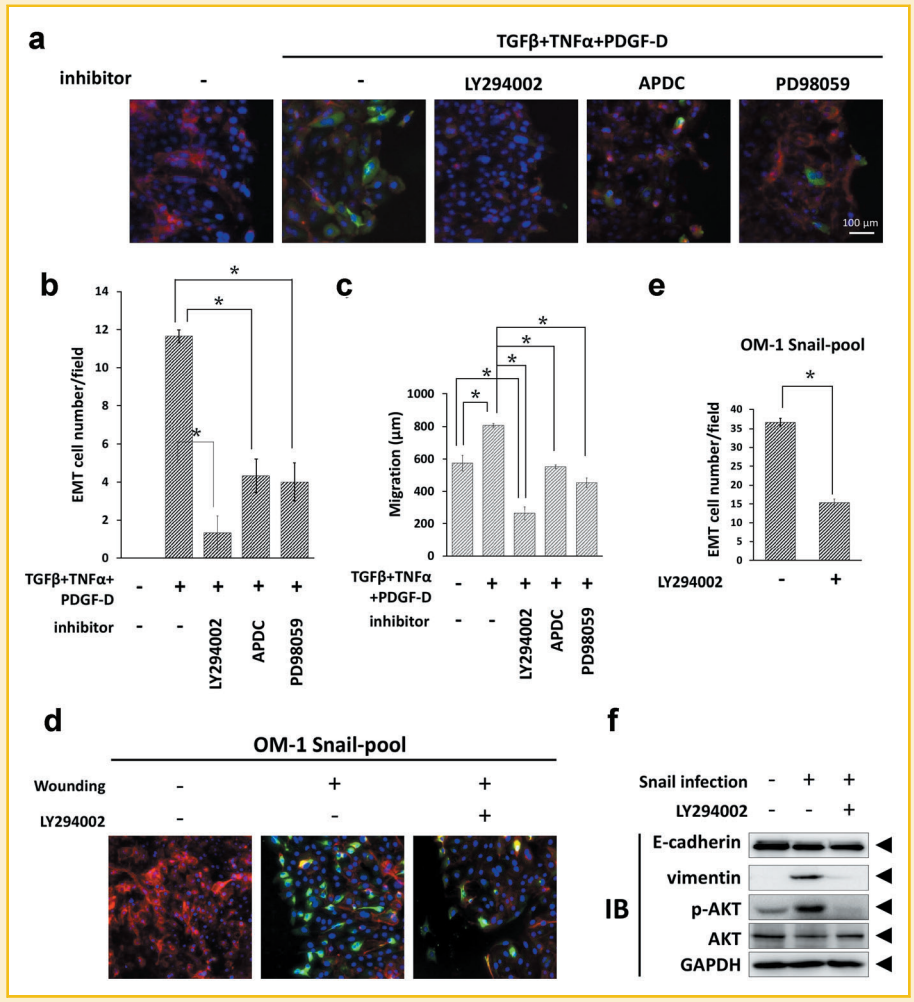

Figure 6. EMT coincides with PI3K–dependent migration of OM–1 cells in a confluent monolayer together with upregulation of Snail and Slug. a: Immunocytochemical analysis of a wounded confluent monolayer of OM1 cells after combined stimulation with TGFβ, TNFα, and PDGF–D for 24 h. PI3K inhibitor LY294002 (50 μM), MEK inhibitor PD98059 (20 μM) or NF–kB inhibitor APDC (20 μM) were added to confluent cultures of OM–1 cells at 1 h prior to stimulation with cytokines and wounding (red: E–cadherin; green: vimentin; blue: nuclei). b: The EMT cell number in (a) was determined by counting the cells undergoing EMT. Data are represented as the means of six independent fields. Error bars represent the SE. $^{*}P < 0.01$, Tukey's test. c: Statistical analysis of cell migration in the same monolayer of OM–1 cells shown in (a). Data are represented as the means of six independent fields. Error bars represent the SE. $^{*}P < 0.01$, Tukey's test. d: Immunocytochemical analysis of a confluent monolayer of OM–1 Snail pool cells at 24 h after wounding. PI3K inhibitor LY294002 (50 μM) was added to confluent monolayers at 1 h prior to wounding (red: E–cadherin; green: vimentin; blue: nuclei). e: EMT cell number in (d) was determined by counting the number of cells undergoing EMT. Data are represented as the means of six independent fields. Error bars represent the SE. $^{*}P < 0.01$, Student's *t*–test. f: Whole cell lysates from cells treated as described in (d) were analyzed by immunoblotting with the indicated antibodies. Densitometric analysis with statistical evaluation among three independent immunoblots is displayed in Supplementary Figure 2d.

plasticity that enables them to undergo phenotypic changes including EMT.

We previously demonstrated that SCC cells acquire a constitutive and irreversible EMT phenotype via the exogenous expression of Snail [Yokoyama et al., 2003]. When we used freshly prepared OM-1 Snail pool cells in the present study, cells that underwent EMT migrated freely around colony islands formed by cells via epithelial homophilic interactions (Fig. 1a), indicating that Snail expression alone was not sufficient to execute the EMT program in all cells harboring the Snail transgene. This theory was further supported by the disappearance of emerging EMT cells from monolayer culture when the cells became confluent (Fig. 2a). Therefore, Snail-dependent execution of EMT displays conditional plasticity.

Treatment with humoral EMT inducers, TGFβ, TNFα, and PDGF-D [Yang et al., 2006; Takahashi et al., 2010], further confirmed the conditional plasticity of EMT in growing OM1 Snail pool cells (Fig. 2b–d). Treatment with TNFα or PDGF-D induced more cells in the OM-1 Snail pool to undergo EMT than that of treatment with TGFβ, as shown by characteristic downregulation of E-cadherin (Fig. 2d). During this process, we found that TNFα promoted nuclear accumulation of Snail (Fig. 4c) and expression of the Zinc transporter LIV (Supplementary Fig. 3e) that is known to activate zinc-finger proteins including Snail [Yamashita et al., 2004]. Because cytoplasmic Snail was observed in some cells that formed colony islands (Fig. 1b), TNFα may suppress E-cadherin expression via the accumulation of functional Snail in the nucleus. LIV may further contribute to the transcriptional suppression of E-cadherin via Snail

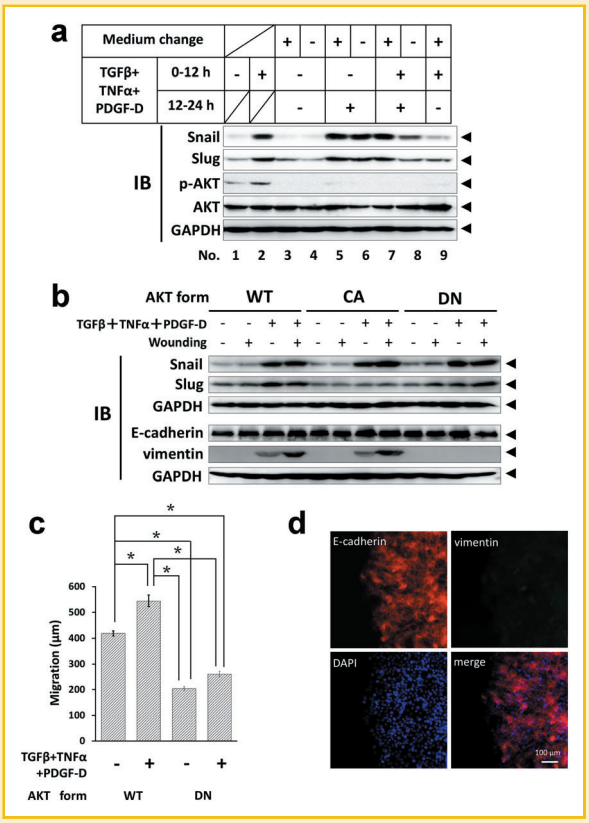

Figure 7. AKT is dispensable for upregulation of Snail and Slug but is essential for EMT concomitant with collective cell motility. a: OM-1 cells were variously treated after wounding. Combined stimulation with TGFβ, TNFα, and PDGF-D was performed at the time of wounding (lanes 2, 7, 8, and 9) or 12 h later (lane 6). The medium was replaced at 12 h after wounding with medium supplemented with (lanes 5 and 7) or without (lanes 3 and 9) the combined cytokines. The cells were harvested at 12 h (lanes 1 and 2) or 24 h (lanes 3–9) after wounding, and whole cell lysates were analyzed by immunoblotting with the indicated antibodies. Densitometric analysis with statistical evaluation among three independent immunoblots is shown in Supplementary Figure 3a and b. b: Confluent monolayers of OM-1 cells harboring wild-type AKT (WT), constitutively active AKT (CA), or dominant negative AKT (DN) were stimulated by TGFβ, TNFα, and PDGF-D with or without wounding. Cell extracts were harvested after 3 h (upper 3 panels) or 6 h (lower 3 panels), and immunoblotting with the indicated antibodies was performed. Densitometric analysis with statistical evaluation among three independent immunoblots is shown in Supplementary Figure 3d. c: Statistical analysis of cell migration in wounded confluent monolayers of OM-1 cells harboring transgenic dominant negative AKT (DN) following combined stimulation with TGFβ, TNFα, and PDGF-D for 24 h. Data are represented as the means of six-independent fields. Error bars represent the SE. $^{*}P < 0.01$, Tukey's test. d: Immunocytochemical analysis of wounded confluent monolayers of OM-1 cells harboring transgenic dominant negative AKT (DN) following combined stimulation with TGFβ, TNFα, and PDGF-D for 24 h (red: E-cadherin; green: vimentin; blue: nuclei).

family proteins because their transcription factor activity is zinc-dependent. Although PDGF-D was also capable of inducing Zeb1 and Zeb2 expression in OM-1 cells (Supplementary Fig. 3f), Zeb1 and Zeb2 were upregulated in cells from the OM-1 Snail pool (Supplementary Fig. 3f) in the absence of cytokine stimulation in SCC clones expressing exogenous Snail [Taki et al., 2006; Taube et al., 2010], suggesting that PDGF-D is of key importance to both Snail-dependent and Zeb-dependent EMT.

In contrast to proliferating cells, all OM-1 Snail pool cells in a confluent monolayer expressed E-cadherin at homophilic cell junctions (Fig. 2a) regardless of the combination of TGFβ, TNFα, and PDGF-D used to stimulate the cells (data not shown). However, creation of new cell-free spaces via narrow wounds in confluent monolayers induced the cells to undergo EMT in the absence of cytokine stimulation (Fig. 6d), indicating that the polarity regained by wounding was also important for execution of the Snail-dependent EMT program.

In contrast to our previous report that demonstrated TGFβ-dependent EMT in growing SCC cells via Zeb2 induction [Taki et al., 2006], treatment with TGFβ alone or combined treatment with TGFβ, TNFα, and PDGF-D did not induce EMT in confluent OM1 cells (Fig. 4a). However, creating a cell-free narrow wound in a confluent monolayer permitted OM-1 cells to undergo EMT at the wound edges in response to combined treatment with TGFβ, TNFα, and PDGF-D (Fig. 3a). Specifically, treatment of confluent monolayers of OM1 cells with TGFβ alone upregulated the expression of both Snail and Slug (Fig. 4b), but not Zeb2 (Supplementary Fig. 3f), suggesting that the growth-arrested confluent condition altered the gene expression profile of cells in response to TGFβ treatment [Arima et al., 2012].

As demonstrated by siRNA-mediated depletion of Snail and Slug, the execution of EMT at wound edges in response to combined stimulation with TGFβ, TNFα, and PDGF-D depended on endogenous Snail and Slug induction (Fig. 5b,c). In this process, PI3K signaling was also essential for Snail/Slug induction (Fig. 3c), cell motility (Fig. 6c), and the execution of EMT (Fig. 6a). In clear contrast, downstream AKT signaling was dispensable for Snail/Slug induction as demonstrated in OM1 cells harboring transgenic AKT-DN (Fig. 7b). However, AKT signaling was essential for cell motility (Fig. 7c), which presumably allowed the Snail/Slug-elevated cells to execute EMT (Fig. 7d) in response to combined stimulation with TGFβ, TNFα, and PDGF-D. PDGF-D appeared to be dispensable for Snail/Slug upregulation (Fig. 4b), but indispensable for EMT (Fig. 4a), whereas TGFβ or TNFα alone were capable of inducing Snail/Slug (Fig. 4b), but incapable of executing the EMT program at the wound edge in a confluent monolayer (Fig. 4a). Therefore, PDGF-D may enable Snail-elevated cells to undergo EMT as a consequence of increasing cell motility via AKT signaling (Fig. 4a,b). The observation that the PI3K inhibitor also prevented cells in the growing OM-1 Snail pool from undergoing EMT (Fig. 6d–f) further confirmed the essential role of AKT signaling in mediating EMT after the acquisition of high Snail expression. Because OM1 cells expressing exogenous Snail gained constitutive AKT activation in the absence of stimulation by TGFβ, TNFα, and PDGF-D (Fig. 6f), an autocrine mechanism may be involved in activation of AKT-dependent motility in EMT. Our previous study showing that several genes, including some secretory factors, are upregulated in response to transgenic Snail [Higashikawa et al., 2008] also supports this idea.

Our present study demonstrates that a Snail/Slug-dependent EMT program with parallel signaling that provides polarized cell motility via AKT is required to execute EMT (Fig. 8d). Our model will contribute to the basic understanding of how varied environmental conditions at a given stage in the cancer life cycle (e.g., stroma invasion vs. nest formation) may induce phenotypic changes (e.g.,

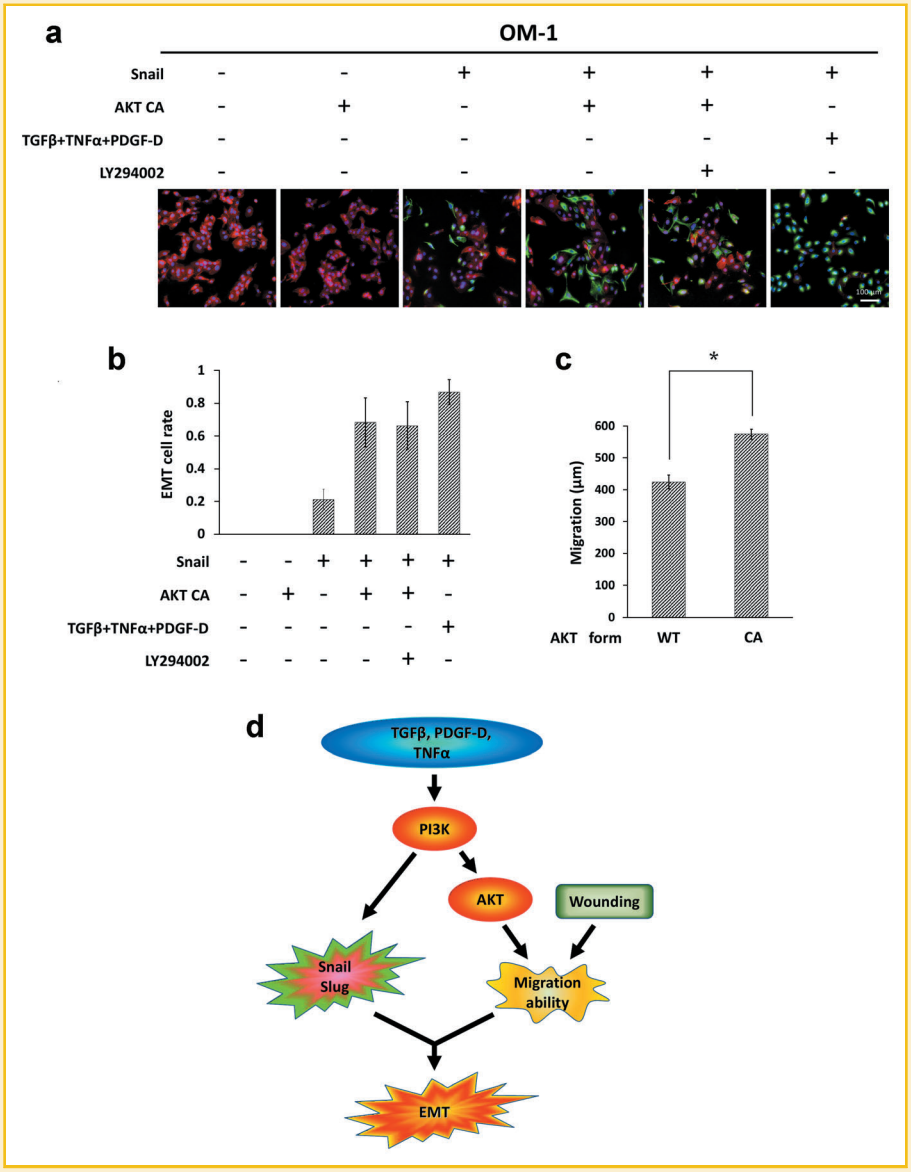

Figure 8. Upregulation of Snail and AKT signaling augments EMT. a: Immunocytochemical analysis of EMT in OM-1, OM-1 Snail pool, and OM-1 AKT-CA cells with the indicated treatments. b: The EMT rate in (a) was determined by counting the total cell number and EMT cells as described in Figure 2c. Each rate is represented as the mean of six independent fields with the SE. c: Statistical analysis of collective cell migration in wound healing assays using AKT-WT and AKT-CA cells. The distance migrated after wounding was measured in phase contrast microscopic views. Data are represented as the means ± SE of six-independent fields. $^{*}P < 0.01$, Student's *t*-test. d: Schematic representation of the pathways that induce EMT in OM-1 cells. PI3K signaling induces Snail family proteins that are not sufficient for initiating EMT. Downstream of PI3K signaling, AKT is dispensable for the upregulation of Snail family proteins but essential for EMT concomitant with collective cell migration of Snail family-elevated cells.

induction of EMT) in SCC cells, even if the EMT master regulator Snail is constitutively expressed at a high level.

ACKNOWLEDGMENTS

We appreciate the valuable discussions with Drs M Taki, K Ohta, T Okumura, and all of our colleagues in the Department of Oral and Maxillofacial Surgery. This work was supported by Grants-in-Aid for Scientific Research (N.K.: 22249066, K.T.: 21791823, and K.H.: 80363084) from the Ministry of Education, Culture, Sports, Science and Technology, Japan.

REFERENCES

Arima Y, Hayashi H, Sasaki M, Hosonaga M, Goto TM, Chiyoda T, Kuninaka S, Shibata T, Ohata H, Nakagama H, Taya Y, Saya H. 2012. Induction of ZEB proteins by inactivation of RB protein is key determinant of mesenchymal phenotype of breast cancer. J Biol Chem 287:7896–7906.

Bakin AV, Tomlinson AK, Bhowmick NA, Moses HL, Arteaga CL. 2000. Phosphatidylinositol 3-kinase function is required for transforming growth factor beta-mediated epithelial to mesenchymal transition and cell migration. J Biol Chem 275:36803–36810.

Barrallo-Gimeno A, Nieto MA. 2005. The Snail genes as inducers of cell movement and survival: Implications in development and cancer. Development 132:3151–3161.

Cano A, Pérez-Moreno MA, Rodrigo I, Locascio A, Blanco MJ, del Barrio MG, Portillo F, Nieto MA. 2000. The transcription factor Snail controls epithelial-mesenchymal transitions by repressing E-cadherin expression. Nat Cell Biol 2:76–83.

Comijn J, Berx G, Vermassen P, Verschueren K, van Grunsven L, Bruyneel E, Mareel M, Huylebroeck D, van Roy F. 2001. The two-handed E box binding zinc finger protein SIP1 downregulates E-cadherin and induces invasion. Mol Cell 7:1267–1278.

Eger A, Aigner K, Sonderegger S, Dampier B, Oehler S, Schreiber M, Berx G, Cano A, Beug H, Foisner R. 2005. DeltaEF1 is a transcriptional repressor of E-cadherin and regulates epithelial plasticity in breast cancer cells. Oncogene 24:2375–2385.

Grünert S, Jechlinger M, Beug H. 2003. Diverse cellular and molecular mechanisms contribute to epithelial plasticity and metastasis. Nat Rev Mol Cell Biol 4:657–665.

Higashikawa K, Yoneda S, Taki M, Shigeishi H, Ono S, Tobiume K, Kamata N. 2008. Gene expression profiling to identify genes associated with high-invasiveness in human squamous cell carcinoma with epithelial-to-mesenchymal transition. Cancer Lett 264:256–264.

Kalluri R, Weinberg RA. 2009. The basics of epithelial-mesenchymal transition. J Clin Invest 119:1420–1428.

LaRochelle WJ, Jeffers M, Corvalan JR, Jia XC, Feng X, Vanegas S, Vickroy JD, Yang XD, Chen F, Gazit G, Mayotte J, Macaluso J, Rittman B, Wu F, Dhanabal M, Herrmann J, Lichenstein HS. 2002. Platelet-derived growth factor D: Tumorigenicity in mice and dysregulated expression in human cancer. Cancer Res 62:2468–2473.

Larue L, Bellacosa A. 2005. Epithelial-mesenchymal transition in development and cancer: Role of phosphatidylinositol 3′ kinase/AKT pathways. Oncogene 24:7443–7454.

Medici D, Hay ED, Goodenough DA. 2006. Cooperation between Snail and LEF-1 transcription factors is essential for TGF-beta1-induced epithelial-mesenchymal transition. Mol Biol Cell 17:1871–1879.

Nieto MA. 2002. The snail superfamily of zinc-finger transcription factors. Nat Rev Mol Cell Biol 3:155–166.

Ramaswamy S, Nakamura N, Vazquez F, Batt DB, Perera S, Roberts TM, Sellers WR. 1999. Regulation of G1 progression by the PTEN tumor suppressor protein is linked to inhibition of the phosphatidylinositol 3-kinase/Akt pathway. Proc Natl Acad Sci USA 96:2110–2115.

Takahashi E, Nagano O, Ishimoto T, Yae T, Suzuki Y, Shinoda T, Nakamura S, Niwa S, Ikeda S, Koga H, Tanihara H, Saya H. 2010. Tumor necrosis factor-alpha regulates transforming growth factor-beta-dependent epithelial-mesenchymal transition by promoting hyaluronan-CD44-moesin interaction. J Biol Chem 285:4060–4073.

Taki M, Kamata N, Yokoyama K, Fujimoto R, Tsutsumi S, Nagayama M. 2003. Down-regulation of Wnt-4 and up-regulation of Wnt-5a expression by epithelial-mesenchymal transition in human squamous carcinoma cells. Cancer Sci 7:593–597.

Taki M, Verschueren K, Yokoyama K, Nagayama M, Kamata N. 2006. Involvement of Ets-1 transcription factor in inducing matrix metalloproteinase-2 expression by epithelial-mesenchymal transition in human squamous carcinoma cells. Int J Oncol 28:487–496.

Taube JH, Herschkowitz JI, Komurov K, Zhou AY, Gupta S, Yang J, Hartwell K, Onder TT, Gupta PB, Evans KW, Hollier BG, Ram PT, Lander ES, Rosen JM, Weinberg RA, Mani SA. 2010. Core epithelial-to-mesenchymal transition interactome gene-expression signature is associated with claudin-low and metaplastic breast cancer subtypes. Proc Natl Acad Sci USA 107:15449–15454.

Thiery JP, Acloque H, Huang RY, Nieto MA. 2009. Epithelial-mesenchymal transitions in development and disease. Cell 139:871–890.

Yamashita S, Miyagi C, Fukada T, Kagara N, Che YS, Hirano T. 2004. Zinc transporter LIVI controls epithelial-mesenchymal transition in zebrafish gastrula organizer. Nature 429:298–302.

Yang L, Lin C, Liu ZR. 2006. P68 RNA helicase mediates PDGF-induced epithelial mesenchymal transition by displacing Axin from beta-catenin. Cell 127:139–155.

Yokoyama K, Kamata N, Hayashi E, Hoteiya T, Ueda N, Fujimoto R, Nagayama M. 2001. Reverse correlation of E-cadherin and snail expression in oral squamous cell carcinoma cells in vitro. Oral Oncol 37:65–71.

Yokoyama K, Kamata N, Fujimoto R, Tsutsumi S, Tomonari M, Taki M, Hosokawa H, Nagayama M. 2003. Increased invasion and matrix metalloproteinase-2 expression by Snail-induced mesenchymal transition in squamous cell carcinomas. Int J Oncol 22:891–898.

Zavadil J, Cermak L, Soto-Nieves N, Böttinger EP. 2004. Integration of TGF-beta/Smad and Jagged1/Notch signalling in epithelial-to-mesenchymal transition. EMBO J 23:1155–1165.

SUPPORTING INFORMATION

Additional supporting information may be found in the online version of this article at the publisher′s website.

Supplementary Figure S1. a: Statistical analysis of protein expression by densitometry in Figure 2d. Data are represented as the means of three independent immunoblots. Error bars represent the SE. $^{*}P < 0.01$, Tukey′s test. b,c: Statistical analysis of protein expression by densitometry in Figure 3c.

Supplementary Figure S2. a,b: Statistical analysis of protein expression by densitometry in Figure 4b. Data are represented as the means of three independent immunoblots. Error bars represent the SE. $^{*}P < 0.01$, Tukey′s test. c: Fold changes of protein expression in Figure 5a. d–f: Statistical analysis of protein expression by densitometry in Figure 6f. Data are represented as the means of three independent immunoblots. Error bars represent the SE. $^{*}P < 0.01$, Tukey′s test.

Supplementary Figure S3. a,b: Fold change analysis of protein expression by densitometry in Figure 7a. Data are represented as the means of three independent immunoblots. Error bars represent the SE. c,d: Fold change analysis of protein expression by densitometry in Figure 7b. Data are represented as the means of three independent immunoblots. Error bars represent the SE. e: Quantitative RT-PCR analysis of Liv-1 mRNA levels in OM-1 cells. TNFα and the known Liv-1 inducer IL-6 were able to induce Liv-1, whereas treatment with an NFkB inhibitor specifically suppressed TNFα-dependent upregulation of Liv-1. f: Evaluation of the mRNA expression levels of Snail, Zeb1 and Zeb2 in OM-1 and OM-1 Snail pool cells in response to the indicated stimuli for 3 h.